

## Check size tuning of the pattern electroretinogram: a reappraisal

MICHAEL BACH<sup>1</sup> & GRAHAM E. HOLDER<sup>2</sup>

<sup>1</sup>*Elektrophysiologisches Labor, Universitäts-Augenklinik, Freiburg, Germany*

<sup>2</sup>*Electrodiagnostic Department, Moorfields Eye Hospital, London, UK*

Accepted 28 May 1996

**Key words:** Check-size, Pattern ERG, PERG, Spatial frequency, Tuning

**Abstract.** The pattern electroretinogram was recorded to checkerboard stimuli with a wide range of check sizes and two stimulus field sizes. Check sizes ranged from 0.25° to 7° (field size, 16° × 14°) and 0.25° to 15° (field size, 32° × 27°) in 14 and seven subjects, respectively. Reversal rate was 4.5/s. For minimal intrusion of blink artifacts the interrupted stimulation technique was employed. The P50 and N95 components of the pattern electroretinogram were evaluated separately. With both stimulus field sizes amplitude of P50 and N95 was maximal between 0.75° and 1°. With smaller check sizes the amplitude dropped monotonically. With larger check sizes field size played a role: with the 16° × 14° field, P50 gradually dropped to 89% from 1° to 7°, which was paralleled by N95 only up to 7°, where N95 dropped to 81% ( $p < 0.05$ ). With the 32° × 27° field, there was no significant difference in size dependency between P50 and N95 for large checks, both components staying constant from 1° to 15°. We conclude that there is only minor large-check attenuation of the pattern electroretinogram, especially with a large field. The apparent field-size dependency may explain previous discrepancies in the literature.

**Abbreviations:** LSFA – low-spatial frequency attenuation.

### Introduction

With the pending publication of the ISCEV guidelines for pattern electroretinogram (PERG) recording, it seems desirable to agree on basic physiologic properties of the PERG and its possible components. Since studies of ganglion cell degeneration [1-4] and current source density studies [5, 6] implicate the retinal ganglion cells in the generation of the PERG, the physiologic properties of the ganglion cells [7] would be expected to be mirrored in the PERG, keeping in mind that the PERG is a mass response averaging responses from various types of cells over the field size stimulated. Thus, on the basis of the lateral inhibition displayed by ganglion cells, many researchers concluded that the PERG should exhibit spatial tuning, or more specifically, low-spatial-frequency attenuation (LSFA). Consequently, responses to large-check stimuli would be derived not from the ganglion

cells, but from nonlinearities of the luminance ERG [8, 9]. However, the experimental findings have been somewhat conflicting.

*The LSFA depends strongly on stimulus parameters.* Conditions that favor spatial selectivity include low luminance, fast sinusoidal modulation in time and space, low contrast and pattern-onset stimulation [10–13]. Conditions that favour a flat tuning curve include high luminance, square-wave modulation in time and space, high contrast and pattern reversal stimulation [4, 14–19].

*Important species differences preclude generalisations from animal models to humans.* In pigeons, the PERG is not affected by ganglion cell loss (optic atrophy) [20]. In cats PERG reduction seems to depend on spatial frequency [21], in monkeys the PERG is extinguished in optic atrophy (spatial frequencies tested, 1–10 cycles/deg) [22] and in humans optic nerve atrophy affects the PERG at all check sizes similarly [3, 4].

One influential line of interpretation examined the possible differences between the two major components of the PERG: the positive excursion at 50 ms (P50) versus the negative excursion at 95 ms (N95). Berninger and Schuurmans [23] reported LSFA for N95 but not for P50, and Holder [24, 25] reported that N95 could be selectively affected in optic nerve or ganglion cell dysfunction, later confirmed by Ryan and Arden [26].

We had so far found conflicting results, namely that Bach and coworkers [13, 27, 28] did not find large-check attenuation with reversal rates of 8/s and less, finding no difference in tuning between P50 and N95; and Holder and coworkers [25, 29, 30, 31] found clinical evidence of dissociation between these components in pathologic conditions. We therefore decided to perform a cooperative experiment, trying to replicate the findings of Berninger and Schuurmans [23] to address this issue in greater detail. As those authors used check sizes up to  $762'$  ( $13^\circ$ ) but used a stimulus field of only  $14.5^\circ \times 18.5^\circ$ , we performed two experiments with two different field sizes, the larger allowing a check size of  $15^\circ$ .

## Subjects and methods

### *Subjects*

Sixteen subjects with normal vision participated in the experiments, 14 in experiment 1 (small field size) and seven in experiment 2 (large field size). Visual acuity was measured in each eye separately before each experiment by optotypes at the same distance as the stimuli, with the automated Freiburg Acuity Test [32]. After appropriate refraction, all subjects reached an acuity of 1.0 or above.

### *Stimuli*

Stimuli were created with a Cambridge Research VSG2 graphics card and displayed on an Eizo 9070S raster-scan display with a frame rate of 70 Hz. Two observation distances were chosen, leading to different stimulus field sizes: Small field: observation distance, 114 cm; stimulus field,  $16^\circ \times 14^\circ$ ; check size,  $0.26^\circ$ ,  $0.52^\circ$ ,  $1^\circ$ ,  $2^\circ$ ,  $4^\circ$  and  $7^\circ$  (actually  $8^\circ \times 7^\circ$ ); and large field: observation distance, 57 cm; stimulus field,  $32^\circ \times 27^\circ$ ; check sizes,  $0.26^\circ$ ,  $0.52^\circ$ ,  $1^\circ$ ,  $2^\circ$ ,  $4^\circ$ ,  $8^\circ$  and  $15^\circ$  (actually  $16^\circ \times 14^\circ$ ).

The checkerboard stimuli were phase reversed at 4.49 reversals per second with a contrast of 98% and a space-averaged mean luminance of  $45 \text{ cd/m}^2$ . Luminance and contrast control of the monitor was calibrated by a method similar to that of Pelli and Zhang [33].

### *Recording*

The PERG signals were picked up by gold foil electrodes simultaneously from the two eyes. The leads were attached to the skin below the eyes with tape and were positioned such that the electrodes did not touch the skin above the tape and avoided, if possible, touching the lower lid. When viewed laterally, a blink from the subject resulted in negligible movement of the electrode. Details of this method have been described previously [34]. While the stimulus was reversing, recording occurred only when a stable baseline was present. Recording was continued for approximately 4 seconds or until instability of the signal baseline was observed. The recording was then interrupted and the subject was asked to blink. Acquisition of data was resumed when the baseline was stable. Artifact rejection occurred whenever the signal exceeded  $\pm 60 \mu\text{V}$ . Periodically or whenever necessary, the subject was asked to sit as still as possible, mouth slightly open (to reduce glossolaryngeal artifacts), head slightly bent forward to raise the gaze slightly (to reduce eye movement noise and to prevent any subject distraction resulting from the gold foil electrode interfering with the view of the stimulus) and to concentrate on the fixation cross in the center of the stimulus. A headrest was used, with the subjects asked to press their head gently backwards on the rest to maintain a stable head position. These technical factors are crucial in obtaining PERGs of low variability [35].

Gold cup reference electrodes were placed at the ipsilateral outer canthi in relation to the zygomatic fossae. This siting for the reference electrode is essential to avoid contamination from the cortically generated VEP. A ground electrode was attached to the forehead. Signals were amplified, filtered (first-order band-pass, 0.32-75 Hz, no notch filter; Toennies Physiological Amplifier) and digitized to a resolution of 12 bits at a sampling interval of 2.33 ms. While generating the stimuli, a computer simultaneously averaged

the sweeps and displayed them on-line, if they were not rejected as artifacts or recording had been paused.

### *Procedure*

Stimuli were presented in a counterbalanced interleaved block design: 30 sweeps to a given check size were obtained, then a different check size was applied. The initial four responses to a new check size were discarded. When all seven or eight check sizes had been presented, the cycle repeated, averaging the results to each individual check size with those previously obtained. This was repeated seven times, leading to a total of  $7 \times 30 = 210$  acquired sweeps per condition. To confirm reproducibility, this procedure was carried out twice in each subject. Thus, two averages composed of 210 sweeps each were obtained for all check sizes and both field sizes.

### *Data analysis*

The final waveforms were digitally phase-free low-pass filtered with a cut-off frequency of 45 Hz. They were averaged for each subject across the two trials and across the two eyes. The N35, P50 and N95 components were then identified interactively. Peak-to-peak amplitude measurements were taken with P50 being measured from N35 to P50, and N95 being measured from P50 to N95.

For grand mean waveforms, we calculated the average together with the standard error of the mean (SEM) for each sample point across subjects. For the sample size ( $n$ ) we used the number of subjects, not the number of eyes.

## **Results**

Figure 1 displays traces from one subject for two check sizes ( $0.52^\circ$  and  $16^\circ$ ). The two traces for each condition are highly reproducible, with minimal trial-to-trial variability. The P50 and N95 amplitudes are identified by arrows.

Figure 2 displays the grand mean of all subjects for all check sizes and the two stimulus sizes (small field at left, large field at right). The thin traces indicate the SEM. For both field sizes the P50 and N95 components are easily identified. The large field produces slightly larger amplitudes. There is an obvious decrease in amplitude of both components at very small check sizes. Toward large check sizes the changes are more subtle. Latency of the P50 component decreases monotonously with increasing check size. This was observed for both field sizes.

Figure 3 shows the relationship between PERG component amplitudes and check size. In addition to the P50 and the N95 components, the ratio N95:P50 is also shown. With the small field, P50 had a maximum at  $1^\circ$

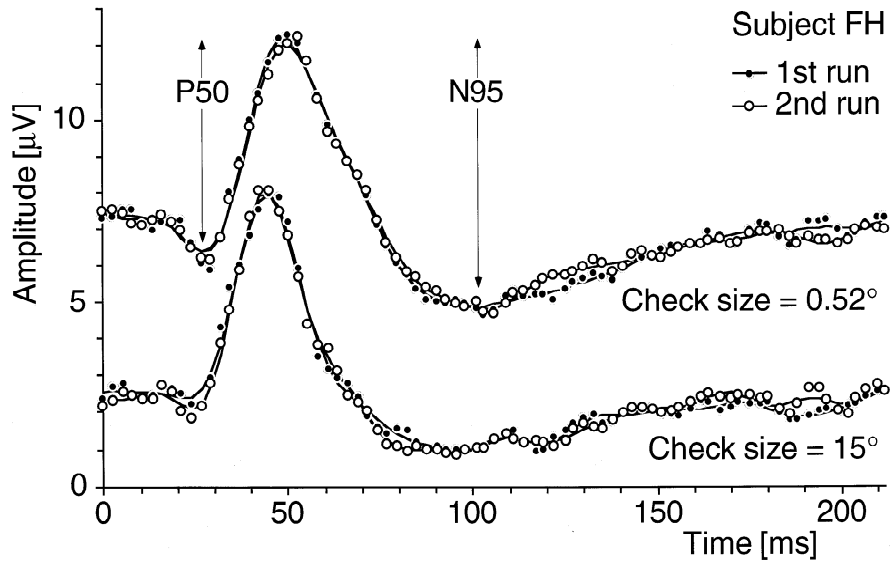


Figure 1. Reproducibility. Symbols represent original data points; the smooth lines represent the outcome of digital filtering with a low-pass cutoff at 45 Hz. The two runs per check size match each other closely.

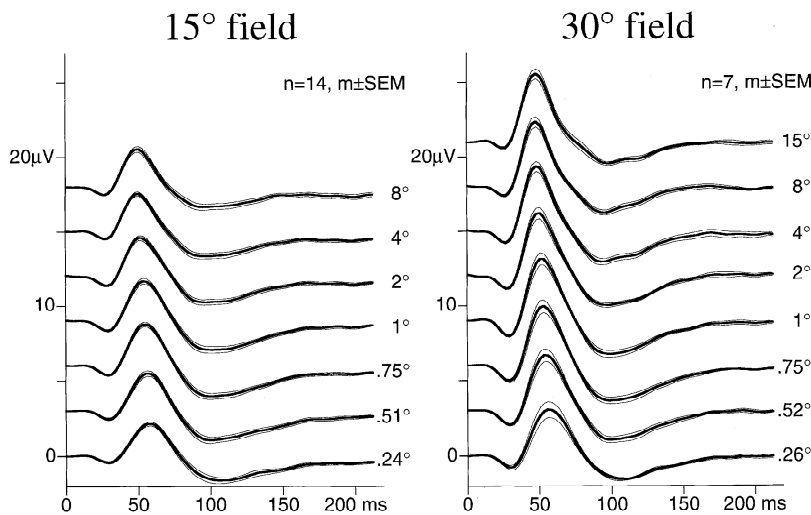


Figure 2. Grand mean traces for the two field sizes and all check sizes, averaged over all subjects (after preaveraging over replications and eyes per subject). Check size increases from bottom to top.

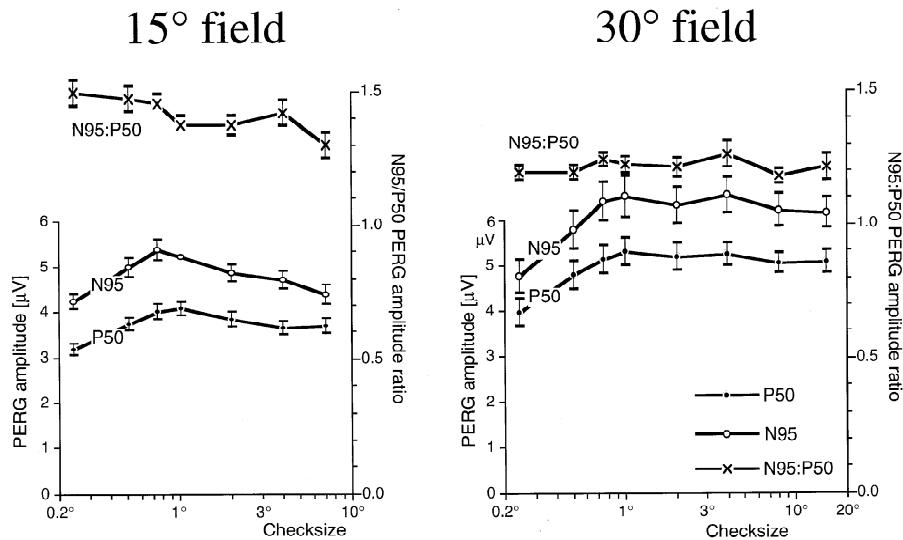


Figure 3. Check size dependency of P50, N95 and N95:P50 ratio at the two field sizes; average  $\pm$  SEM of individually detected peaks over subjects. Maximal amplitude is observed between  $0.75^\circ$  and  $1^\circ$  of check size. Some large check attenuation is apparent for the small field. (left), virtually none for the large field (right). For the small field, the N95:P50 ratio shows a shallow decline with increasing check size.

gradually dropping to 89% from  $1^\circ$  to  $7^\circ$ ; N95 had a maximum at  $0.75^\circ$ , dropping down to 81% at  $7^\circ$  ( $p < 0.05$ ). The N95:P50 ratio dropped from 1.5 to 1.3 with increasing check size. With the large field, both P50 and N95 had their maximum at  $1^\circ$ . Although one larger check size than with the small field was possible, the slight attenuation for large checks (96% for P50, 94% for N95) was not statistically significant. The N95:P50 ratio was nearly constant.

## Discussion

Well-defined and highly reproducible PERG responses were recorded in all subjects and for all check sizes. With regard to the experimental variables check size and stimulus field, we found the following.

1. At the small check side branch, PERG amplitude diminishes below  $0.5^\circ$ . This is a well-known phenomenon, which probably results from two factors. First, space-averaged over the stimulus field, checks become smaller than the receptive field centers, leading to submaximal excitation of the ganglion cells. Second, the contrast of the retinal image is degraded with decreasing check size because of the limited bandwidth of the modulation transfer factor of the optics of the eye [36, 37].

2. Maximal PERG amplitude occurs for check sizes of  $0.75^\circ$  for both the  $16^\circ \times 14^\circ$  and  $32^\circ \times 27^\circ$  stimulus field. This supports the current suggestion of a check size of  $0.75^\circ$  in the ISCEV PERG guidelines [38].

3. For the  $16^\circ \times 14^\circ$  small stimulus field, both P50 and N95 show a moderate attenuation down to 89% and 81% respectively at a check size of  $7^\circ$  relative to the maximum at  $0.75^\circ$ . For the  $32^\circ \times 27^\circ$  large stimulus field, neither P50 nor N95 show appreciable low-spatial-frequency attenuation, even though larger checks were possible than with the smaller stimulus field.

4. A small (87%) but significant difference occurs between the N95 and the P50 tuning in the small stimulus field condition, N95 being more affected than P50. No significant difference occurs between the N95 and the P50 tuning in the large field condition.

5. Latency of the P50 component decreases monotonously with increasing check size, as previously reported by Arden et al. [15].

The results are in agreement with previous reports [4, 14, 19, 39]. However, they disagree with the findings of Berninger and Schuurmans [23], although the stimulus conditions were similar. The most striking difference was obtained for the  $15^\circ$  check condition, where the present study found the amplitude of both P50 and N95 to be within 96%/94% of maximum, while Berninger and Schuurmans [23] found a drop down to 58% for N95. Personal communication with the authors revealed that in their largest check condition, only the left top check was of full size, while the others were clipped by their  $14.5^\circ \times 18.5^\circ$  monitor size. This is a suboptimal stimulus definition, and we presume that the current results may be more reliable. The effect of field size has been noted before: Vaegan and Arden [40] compared two field sizes ( $4.7 \times 7.5^\circ$  versus  $14^\circ$  diameter) and found stronger LSFA for the smaller field size. It may in part be related to the change of receptive field sizes with eccentricity [41].

Spatial tuning has often been considered evidence to link the PERG to ganglion cell activity. However, a checkerboard stimulus, while clinically useful, may not be most appropriate to address this question. (1) A checkerboard is composed of multiple spatial frequencies. (2) Rapid pattern reversal (square-wave in time) inherently stimulates both transient and sustained mechanisms, which will mix in an unknown way in the recorded mass response. (3) Various physiologic properties vary with eccentricity, and associated responses are integrated over the entire stimulus field in the PERG. Although the PERG (both P50 and N95) may be derived from the ganglion cells (see Introduction), this does not mean that the same type of ganglion cell necessarily generates the PERG for different check sizes. It is more likely that multiple mechanisms generate the PERG and the relative weight of these mechanisms changes with change in check size (for example, Bach et al. [27]) and other

stimulus parameters. In this light it seems possible that the differential effect of retinal or optic nerve pathology on P50 and N95 [24, 25] may vary with field size. While no systematic study has tackled this problem to date, it seems possible that the differential effect will be more pronounced with relatively small stimulus fields ( $15^\circ$  diameter or less). If this were indeed found to be the case, it becomes an important contributory factor in the design of stimulus paradigms for optimum clinical sensitivity.

### Acknowledgment

This work was supported by the Deutsche Forschungsgemeinschaft (SFB 325, B3) and by the Meyer-Schwartz-Stiftung.

### References

1. Groneberg A, Teping C. Topodiagnostik von Sehstörungen durch Ableitung retinaler und kortikaler Antworten auf Umkehr-Kontrastmuster. *Ber Dtsch Ophthalmol Ges* 1980; 77: 409–15.
2. Maffei L, Fiorentini A. Electroretinographic responses to alternating gratings before and after section of the optic nerve. *Science* 1981; 211: 953–4.
3. Harrison JM, O'Connor PS, Young RSL, Kincaid M, Bentley R. The pattern ERG in man following surgical resection of the optic nerve. *Invest Ophthalmol Vis Sci* 1987; 28: 492–9.
4. Bach M, Gerling J, Geiger K. Optic atrophy reduces the pattern-electroretinogram for both fine and coarse stimulus patterns. *Clin Vision Sci* 1992; 7: 327–33.
5. Sieving PA, Steinberg RH. Proximal retinal contributions to the intraretinal 8-Hz pattern ERG of cat. *J Neurophysiol* 1987; 57: 104–20.
6. Baker CL, Hess RF, Olsen BT, Zrenner E. Current source density analysis of linear and non-linear components of the primate electroretinogram. *J Physiol* 1988; 407: 155–76.
7. Enroth-Cugell C, Robson JG. Functional characteristics and diversity of cat retinal ganglion cells: basic characteristics and quantitative description. *Invest Ophthalmol Vis Sci* 1. 84; 25: 250–67.
8. Maffei L. Electroretinographic and visual cortical potentials in response to alternating gratings. *Ann NY Acad Sci* 1982; 388: 1–10.
9. Riemsdag FCC, Ringo JL, Spekrijse H, Verduyn Lunel H. The distinction between luminance and spatial contrast components in the pattern ERG. *Doc Ophthalmol Proc Ser* 1983; 37: 255–64.
10. Korth M. Pattern-evoked responses and luminance-evoked responses in the human electroretinogram. *J Physiol* 1983; 337: 451–69.
11. Hess RF, Baker CL. Human pattern-evoked electroretinogram. *J Neurophysiol* 1984; 51: 939–51.
12. Korth M, Rix R. Changes in spatial selectivity of pattern-ERG components with stimulus contrast. *Graefes Arch Clin Exp Ophthalmol* 1985; 223: 23–8.
13. Bach M, Speidel-Fiaux A. Pattern electroretinogram in glaucoma and ocular hypertension. *Doc Ophthalmol* 1989; 73: 173–81.
14. Korth M. Human fast retinal potentials and the spatial properties of a visual stimulus. *Vision Res* 1981; 21: 627–30.

15. Arden GB, Vaegan, Hogg CR. Clinical and experimental evidence that the pattern electroretinogram (PERG) is generated in more proximal retinal layers than the focal ERG (FERG). *Ann NY Acad Sci* 1982; 388: 580–607.
16. Kirkham TH, Coupland SG. Pattern ERGs and check size: absence of spatial frequency tuning. *Curr Eye Res* 1982; 2: 511–21.
17. Trick GL, Wintermeyer DH. Spatial and temporal frequency tuning of pattern-reversal retinal potentials. *Invest Ophthalmol Vis Sci* 1982; 23: 774–9.
18. Vaegan, Arden GB, Hogg CR. Properties of normal electroretinograms evoked by patterned stimuli in man. *Doc Ophthalmol Proc Ser* 1982; 31: 111–29.
19. Sokol S, Jones K, Nadler D. Comparison of spatial properties of human retina and cortex as measured by simultaneously recorded pattern ERGs and VEPs. *Vision Res* 1983; 23: 723–7.
20. Porciatti V, Francesconi W, Bagnoli P. The pigeon pattern electroretinogram is not affected by massive loss of cell bodies in the ganglion layer induced by chronic section of the optic nerve. *Doc Ophthalmol* 1985; 61: 41–7.
21. Tobimatsu S, Celesia GG, Cone S, Gujrati M. Electroretinograms to checkerboard pattern reversal in cats: physiological characteristics and effect of retrograde degeneration of ganglion cells. *Electroencephalog Clin Neurol* 1989; 73: 341–52.
22. Holländer H, Bisti S, Maffei L, Hebel R. Electroretinographic responses and retrograde: changes after intracranial optic nerve section: a quantitative analysis in the cat. *Exp Brain Res* 1984; 55: 483–493.
23. Berninger T, Schuurmans RP. Spatial tuning of the pattern ERG across temporal frequency. *Doc Ophthalmol* 1985; 61: 17–25.
24. Holder GE. Pattern ERG abnormalities in anterior visual pathway disease. *Electroencephalog Clin Neurophysiol* 1985; 61: S135.
25. Holder GE. Significance of abnormal pattern electroretinography in anterior visual pathway dysfunction. *Br J Ophthalmol* 1987; 71: 166–71.
26. Ryan S, Arden GB. Electrophysiological discrimination between retinal and optic nerve disorders. *Doc Ophthalmol* 1988; 68: 247–55.
27. Bach M, Hiss P, Röver J. Check-size specific changes of pattern electroretinogram in patients with early open-angle glaucoma. *Doc Ophthalmol* 1988; 69: 315–22.
28. Bach M, Gerling J. Retinal and cortical activity in human subjects during color flicker fusion. *Vision Res* 1992; 32: 1219–23.
29. Holder GE. The incidence of abnormal pattern electroretinography in optic nerve demyelination. *Electroencephalog Clin Neurophysiol* 1991; 78: 18–26.
30. Holder GE. Pattern electroretinography in the evaluation of glaucoma and in optic nerve function. In: Heckenlively JR, Arden GB (eds.) *Principles and practice of clinical electrophysiology of vision*. St. Louis: Mosby–Year Book, 1991: 549–56.
31. Manguiere F, Holder GE, Luxon LM, Pottinger R. Evoked potentials: abnormal waveforms and diagnostic yield of evoked potentials. In: Osselton J, Binnie CD, Cooper R, Fowler CJ, Manguiere F, Prior PF, (eds.) *Clinical neurophysiology: EMG, nerve conduction and evoked potentials*. Oxford: Butterworth-Heine 1995: 431–81.
32. Bach M. The Freiburg Visual Acuity Test – Automatic measurement of visual acuity. *Optometry Vision Sci.* 1996; 73: 49–53
33. Pelli DG, Zhang L. Accurate control of contrast on microcomputer displays. *Vision Res* 1991; 31: 1337–50.
34. Holder GE. Recording the pattern electroretinogram with the Arden gold foil electrode. *J Electrophysiol Technol* 1988; 14: 183–90.
35. Odom JV, Holder GE, Feghali JG, Cavender S. Pattern electroretinogram intrasession reliability: a two center comparison. *Clin Vis Sci* 1992; 7: 263–282.
36. Drasdo N, Thompson DA, Thompson CM, Edwards L. Complementary components and local variations of the pattern electroretinogram. *Invest Ophthalmol Vis Sci* 1987; 28: 158–62.

37. van den Berg TJTP, Boltjes B. The point-spread function of the eye from 0° to 100° and the pattern electroretinogram. *Doc Ophthalmol* 1988; 67: 347–54.
38. Marmor M, Holder GE, Porciatti V, Trick GL Zrenner E. ISCEV PERG guidelines. *Doc Ophthalmol*. In press.
39. Vaegan, Arden GB. Effect of pattern luminance profile on the pattern ERG in man and pigeon. *Vision Res* 1987; 27: 883–92.
40. Vaegan, Arden GB. Electroretinograms evoked in man by local uniform or unpatterned stimulation. *J Physiol* 1983; 341: 85–104.
41. Kelly DHC. Spatial frequency selectivity in the retina. *Vision Res* 1975; 15: 665–72.

*Address for correspondence:* M. Bach, Universitäts-Augenklinik, Killianstr. 5, D-79106 Freiburg, Germany  
Phone ++49-(761) 270-4060/4061; Fax: ++49-(761) 270-4104; e-mail: bach@uni-freiburg.de